Electronic Supplementary Material (ESI) for RSC Advances.

One-pot synthesis of polyaniline-gold nanocomposite and its enhanced electrochemical properties for biosensing application

Amrita Soni, Chandra Mouli Pandey, Shipra Solanki, Gajjala Sumana
Biomedical Instrumentation Section, CSIR-National Physical Laboratory, New Delhi-110012, India.

Supporting information

Figure S1. DLS measurements representing (a) particle size distribution of AuNPs. (b)zeta potential values of AuNPs (c) zeta potential values of PANI-Au nanocomposite synthesized by chemical route.

Figure S2. BET surface area analysis of (i) EC-PANI-Au nanocomposite (ii) PANI-Au nanocomposite synthesized by chemical route.

Figure S3. FT-IR spectra of (a) PANI/ITO electrode (b) EPD-PANI-Au/ITO electrode (c) pDNA/EPD-PANI-Au/ITO bioelectrode.

Figure S4. Cyclic voltammetric analysis of (a) (i) bare ITO (ii) pDNA/EPD-PANI-Au/ITO electrode (iii) pDNA/EC-PANI-Au/ITO electrode (iv) EPD-PANI-Au/ITO (v) EC-PANI-Au/ITO at 50 mVs^{-1}. CV analysis of (b) EPD-PANI-Au/ITO electrode (c) EC-PANI-Au/ITO electrode with varying scan rates in PBS (100 mM, pH 7.0, 0.9% NaCl) containing 5 mM $[Fe(CN)_6]^{3-/4-}$. Inset figures show linearity plot of the peak current values as a function of square root of scan rate and the plot of peak potential values as a function of log of scan rate.

Figure S5. (a) Percentage change in hybridization efficiency for pDNA/EPD-PANI-Au/ITO biolelectrode with repeated denaturation and rehybridization process. (b) Stability of the electrode after 14 weeks.

Figure S1.

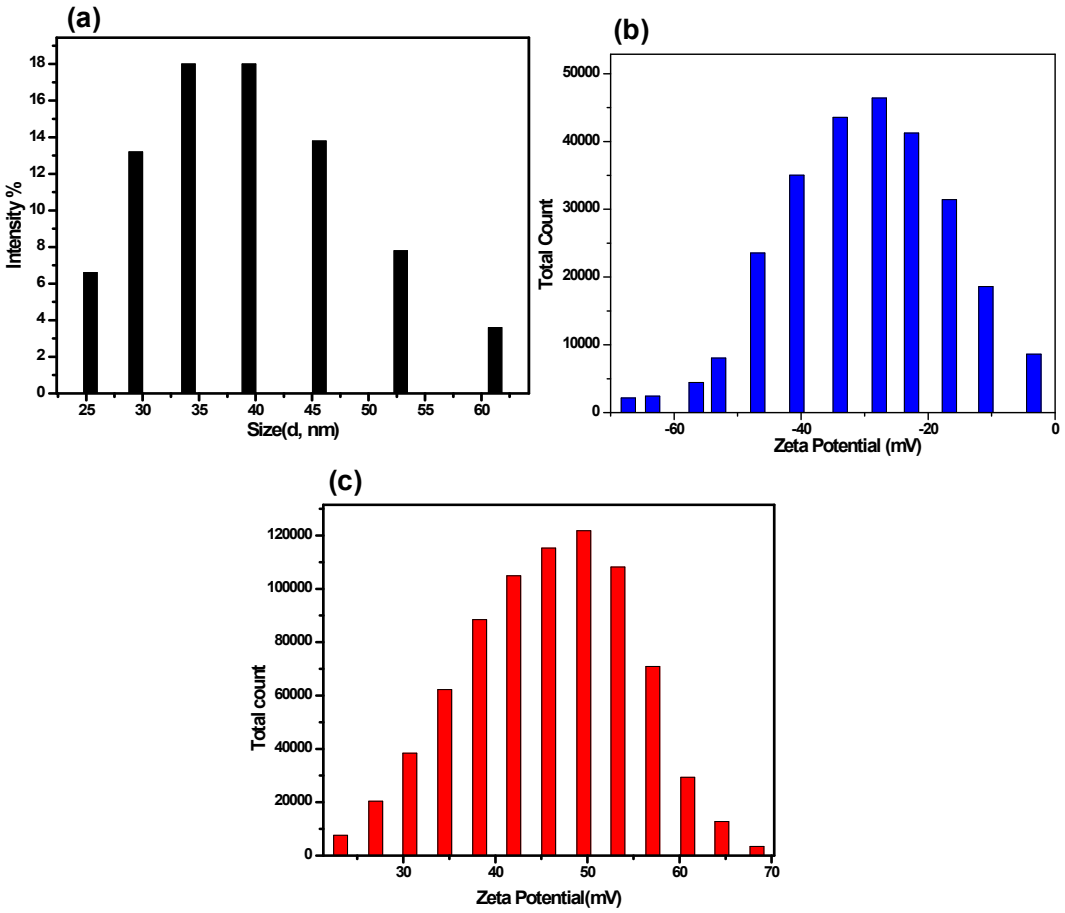

Figure S2.

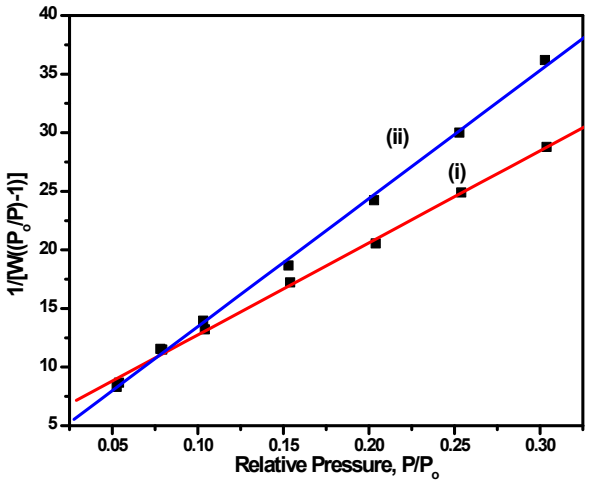

Figure S3.

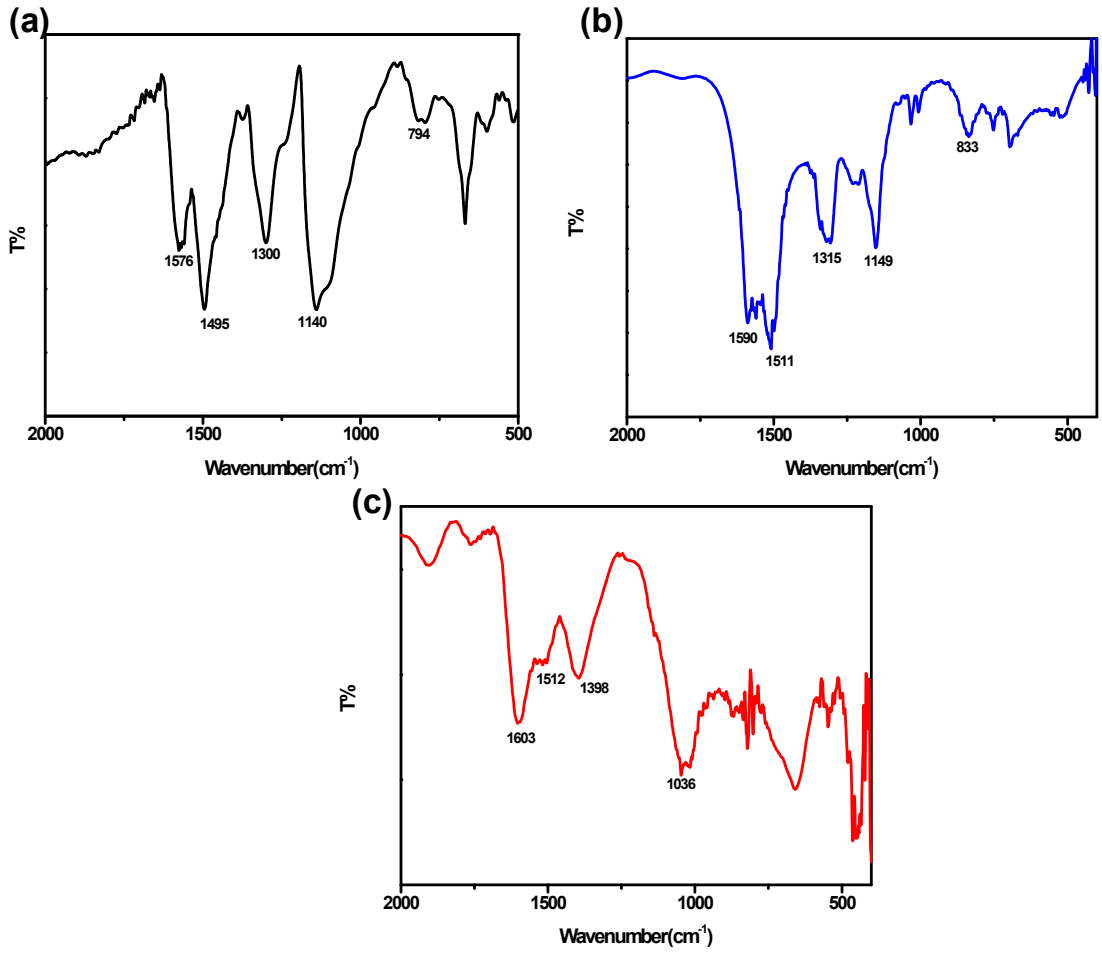
(a)
T%
1576
1495
1300
1140
794
2000
1500
1000
500
Wavenumber(cm-1)
(b)
T%
1590
1511
1315
1149
833
2000
1500
1000
500
Wavenumber(cm-1)
(c)
T%
1603
1512
1398
1036
2000
1500
1000
500
Wavenumber(cm-1)

Figure S4.

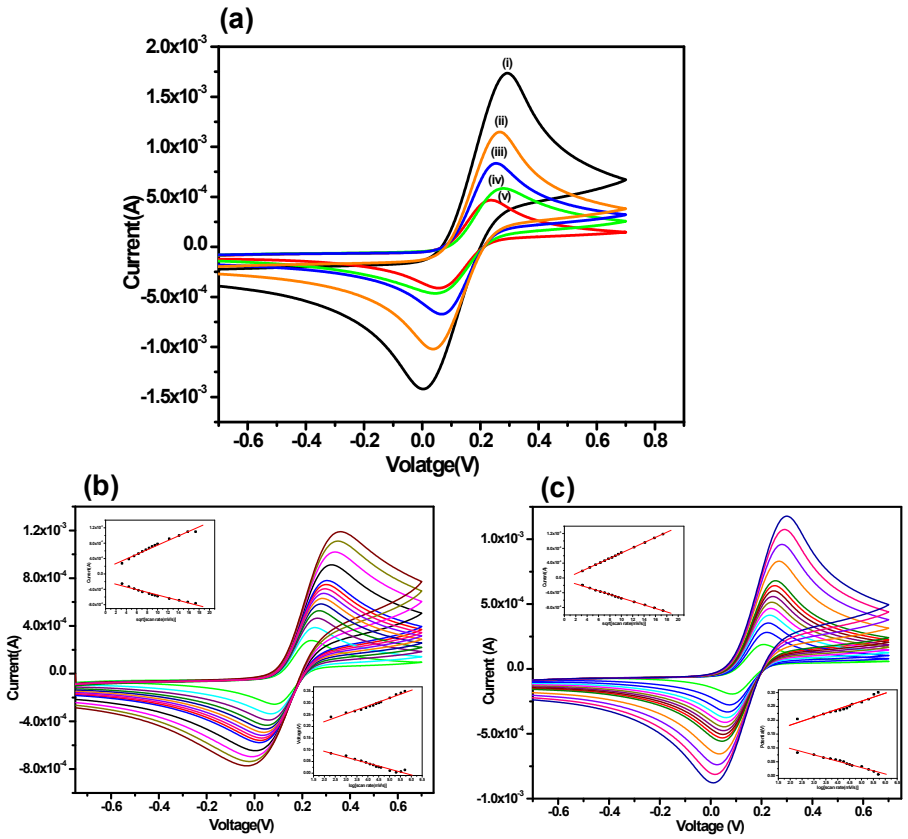

Figure S5.